

Electrochemical Switching Fluorescence Emission in Rhodamine Derivatives

Martina Čížková, Laurent Cattiaux, Jean-Maurice Mallet, Eric Labbé, Olivier Buriez

▶ **To cite this version:**

Martina Čížková, Laurent Cattiaux, Jean-Maurice Mallet, Eric Labbé, Olivier Buriez. Electrochemical Switching Fluorescence Emission in Rhodamine Derivatives. Electrochimica Acta, 2018. hal-01684343

HAL Id: hal-01684343
https://ens.hal.science/hal-01684343

Submitted on 15 Jan 2018

HAL is a multi-disciplinary open access archive for the deposit and dissemination of scientific research documents, whether they are published or not. The documents may come from teaching and research institutions in France or abroad, or from public or private research centers.

L'archive ouverte pluridisciplinaire **HAL**, est destinée au dépôt et à la diffusion de documents scientifiques de niveau recherche, publiés ou non, émanant des établissements d'enseignement et de recherche français ou étrangers, des laboratoires publics ou privés.

Electrochemical Switching Fluorescence Emission in Rhodamine Derivatives

Martina Čížková,[a] Laurent Cattiaux,[b] Jean-Maurice Mallet,[b] Eric Labbé,[a] and Olivier Buriez*[a]

[a] PASTEUR, Département de chimie, École normale supérieure, PSL Research University, Sorbonne Universités, UPMC Univ. Paris 06, CNRS, 75005 Paris, France.

[b] Laboratoire des Biomolécules, Département de chimie, École normale supérieure, PSL Research University, Sorbonne Universités, UPMC Univ. Paris 06, CNRS, 24 rue Lhomond, 75005 Paris, France.

Abstract

Three rhodamine derivatives exhibiting electrofluorochromic properties were investigated by cyclic voltammetry and UV-Vis/fluorescence spectroelectrochemistry. Rhodamine 101 (Rh101, compound **1**) was used as a reference model. In compound **2**, the carboxylate anion of Rh101 was replaced by an alkyne moiety to allow further functionalization. The compound **3** was prepared from **2** by conversion of the alkyne to a triazole group bearing an alkyl chain with an alcohol function. These three rhodamine derivatives exhibited similar electrochemical behaviors. Their mono-electronic reductions produced the corresponding radical species which were stable on the time-scale of cyclic voltammetry. Additional reduction of electrogenerated radicals produced unstable anions which underwent subsequent chemical reaction, most likely protonation. Based on cyclic voltammetry investigations, absorption and fluorescence spectroelectrochemistry were then performed on compounds **1**, **2**, **3** and their parent reduced radicals **1a**, **2a**, **3a**. UV-Vis spectroelectrochemistry, combined with TD-DFT calculation, confirmed the formation of radicals upon mono-electronic reduction of starting rhodamines. Fluorescence spectroelectrochemistry showed that, contrary to their parent molecules, electrogenerated radicals were non-fluorescent. Electrochemical fluorescence extinction was successfully achieved with all studied compounds. Moreover, compound **1** underwent on/off switching between fluorescent and non-fluorescent states repeatedly. Also, recovery of fluorescence in compound **3** was observed, which open interesting opportunities for the development of versatile rhodamine-based probes.

1. Introduction

Combination of electrochemistry with spectroscopic techniques is a powerful tool in the fields of analytical chemistry, biophysics and chemical physics. Especially electrofluorochromism, in which fluorescence of molecules can be modulated electrochemically, is becoming a very attractive approach in analytical and bioanalytical chemistry since many analytes are redox active and can be detected and/or mapped with high sensitivity through fluorescence[1, 2]. Even though electrochemical fluorescence modulation is becoming a promising approach, only a few systems based on single fluorescent molecules [3-7], molecular dyads [8-10], or polymers [11] have been described. The use of intrinsically switchable fluorophores appears to be the most straightforward strategy as the fluorophore can behave both as the light emitter and the redox switch. Nevertheless, this strategy is well-adapted only if the electrogenerated ion-radicals are stable enough. Accordingly, compounds possessing extended π-electron systems such as rhodamine derivatives are good candidates. Rhodamine derivatives, which belong to the family of xanthenes, are widely used as fluorescent probes owing to their high absorption coefficients, high quantum yields and photostability [12, 13]. Furthermore, fluorescent markers emitting in red are extremely valuable in biological microscopy since they minimize cellular auto-fluorescence and increase flexibility in multicolor experiments [14, 15]. Within the rhodamine family, Rh101 is one of the most stable fluorophores with a quantum yield close to unity which can be used as a reference substance for fluorescence quantum yield measurements [16]. Interestingly, fluorescence of Rh101 was found to be quenched by amine derivatives [17] or by graphene oxide [18], but the quenching was found to be irreversible. Fluorescence of Rh101 was also found to be switchable when the fluorophore was grafted to a photochromic compound. In this case, fluorescence was reversibly quenched by focused light [19]. However, to the best of our knowledge the fluorescence quenching of Rh101 has never been investigated by electrochemistry, although some electrochemical investigations of several rhodamine derivatives, such as rhodamine B and rhodamine 6G, have been reported [20-23]. Rhodamine B was especially investigated for its photoelectrochemical properties. In 1974, Krüger and Memming reported on the photoelectrochemistry of rhodamine B using conducting SnO_2 film electrodes [23]. Under these conditions, the reduction of rhodamine B was shown to first lead to a radical anion, which then formed a complex with rhodamine B. Disproportionation of the one-electron reduced rhodamine B into rhodamine B and leuco-rhodamine B was expected, but not observed. In 1986, Quickenden *et al.* reported on the power conversion efficiency of the rhodamine B photoelectrochemical cell containing unmodified and electrochemically modified SnO_2 glass photoelectrodes [21]. In 2010, F. Marken *et al.* used rhodamine B as a photoactive redox system to investigate photoelectrochemical processes at a liquid/liquid/solid electrode interface [20]. Microdroplets of the water-immiscible 3-(4-phenylpropyl)-pyridine containing rhodamine B were deposited onto a basal plane pyrolytic graphite electrode surface which was then immersed into an aqueous solution containing a phosphate buffer solution (pH 12). Under these conditions, and in the absence of light, it was shown that reduction of rhodamine B involved two steps (both one-electron processes) whereas the re-oxidation occurred through a single two-electron process. Voltammetric signals were consistent with sodium cation transfer (for the first reduction step) and proton transfer (for the second reduction step) coupled to the electron transfer.

Rhodamine 6G (R6G) was also investigated electrochemically. It was notably shown that the electrochemical reduction of R6G at a bare electrode, in aqueous solution, led to an irreversible reduction process due to a strong adsorption of R6G on the electrode surface [22]. Nevertheless, it was reported that modification of the electrode surface with 4,4'-bipyridyl led to a quasi-reversible one-electron reduction process.

Herein, three rhodamine derivatives, including the commercially available Rh101 and two novel derivatives (Scheme 1), were investigated by cyclic voltammetry and UV-Vis/fluorescence spectroelectrochemistry. We established that the fluorescence switching of Rh101 can be achieved electrochemically. This result prompted us to carry out the functionalization of the Rh101 molecule and examine whether the electrochemical fluorescence switching were preserved on the resulting compounds. Accordingly, an original rhodamine derivative **2** bearing an alkyne moiety was first prepared (Scheme 1), then used to synthesize the triazole derivative **3** (Scheme 1).

< Scheme 1>

2. Experimental Section

2.1. Materials

Compounds for the synthesis of compound **2** and **3** were used as received: CF_3COOH (Carlo Erba P0082746), CH_2Cl_2 (Carlo Erba 528461), $CuSO_4$ (Alfa Aesar A11262), cyclohexane (Carlo Erba 528215), DMF (Carlo Erba 444926), EDTA (Alfa Aesar A15161), Et_2O (Carlo Erba 447534), EtOAc (Carlo Erba 528295), EtOH (Carlo Erba 528151), HCl (VWR 20252.324), H_2O (distilled with Aquatron® model A4000), 8-hydroxyjulolidine (Sigma Aldrich 249394), K_2CO_3 (Alfa Aesar A16625), MeOH (Carlo Erba 528101), $MgSO_4$ (VWR 25162.465), NaCl (VWR 27788.460), propargyl bromide (Sigma-Aldrich 81831), rhodamine 101 (compound **1**, Sigma-Aldrich 83694), salicylaldehyde (Sigma-Aldrich S356), silica gel (Macherey-Nagel 815381.1), sodium ascorbate (Sigma-Aldrich 11140), tetrachloro-1,4-benzoquinone (Sigma-Aldrich 232017), trifluoromethane-sulfonic acid (Sigma-Aldrich 158534). 1-Azidopropan-3-ol was previously prepared in our laboratory [24]. Compounds for electrochemical and spectroelectrochemical experiments were also used without further purification: anhydrous MeCN (Sigma-Aldrich 271004), ferrocene (Sigma-Aldrich 46260). Tetrabutylammonium tetrafluoroborate ($TBA.BF_4$) was synthesized from tetrabutylammonium hydrogen sulfate by anion metathesis with sodium tetrafluoroborate. MeOH (Sigma Aldrich 249394) for spectroscopic measurements was used as received.

2.2. Cyclic voltammetry

Cyclic voltammetry (CV) was performed on Autolab PGSTAT 20 potentiostat in a three-electrode electrochemical cell with a 1 mm sized home-made glassy carbon electrode (Goodfellow) used as a working electrode, saturated calomel electrode (SCE, Radiometer) as a reference electrode, and a platinum wire (Goodfellow) as a counter electrode. The reference electrode was separated from the bulk solution by a fritted-glass bridge filled with the solution of supporting electrolyte (0.1 M TBA·BF4 in MeCN). CV experiments were measured after at least 10 min of argon purging, at room temperature, with ferrocene as an internal standard. The half-wave potential of the ferrocene/ferrocenium redox couple (Fc/Fc^+) was 0.420 V/SCE [25].

2.3. Spectroelectrochemical measurements

Spectroelectrochemical experiments were carried out on Autolab PGSTAT 20 potentiostat in a quartz glass spectroelectrochemical cell with 0.5 mm optical path length (Biologic) using platinum mesh as a working electrode, non-aqueous Ag/Ag^+ (Biologic instruments; silver wire soaking in a non-aqueous electrolyte Ag+/MeCN/TBAP (tetrabutyl ammonium perchlorate)) as a reference electrode, and a platinum wire as a counter electrode. The platinum mesh electrode was treated with piranha solution (concentrated sulfuric acid/30% hydrogen peroxide 3:1) before every experiment. Caution: piranha solution is extremely reactive and may result in explosion or skin burns if not handled with extreme care. 0.1 M $TBA{\cdot}BF_4$ in MeCN was used as a supporting electrolyte. Perkin Elmer Lambda 45 spectrometer was used in absorption spectroelectrochemical experiments and JASCO FP-8300 spectrofluorometer in fluorescence spectroelectrochemical experiments. All experiments were performed after at least 10 min of argon purging, at room temperature, with ferrocene as an internal standard. The half-wave potential of the ferrocene/ferrocenium redox couple (Fc/Fc^+) was 0.095 V with the non-aqueous Ag/Ag^+ reference electrode. All potentials were recalculated to SCE by adding the difference of 0.325V to all measured values.

2.4. DFT calculations

The quantum chemical calculations were performed using the Gaussian 09 package [26]. Geometry optimizations were performed with DFT/B3LYP/6-31+g(d,p) level of theory. The presence of local energy minimum in final structures was confirmed by frequency calculation with the same basis set. Absorption spectra were obtained from excited state calculation based on time-dependent density functional theory (TD-DFT) employing the CAM-B3LYP/6-31+g(d,p) level of theory (n states = 30). Absorption spectra were generated by broadening the calculated transition intensities by Gaussian curve with half-width of 0.1 eV and with wavelength scaling of 0.4 eV.

2.5. Syntheses and analytical data

The synthesis of 2-(Prop-2-yn-1-yloxy)benzaldehyde (**4**) (CAS: 29978-83-4) was based on a literature procedure [27] (Scheme 2).

< Scheme 2>

Propargyl bromide (80% in toluene; 10.1 mL, 93.7 mmol) was added slowly over the period of 1 hour to the solution of salicylaldehyde (10.0 g, 81.9 mmol) and K_2CO_3 (12.7 g, 91.9 mmol) in DMF (150 mL). The reaction was stirred at room temperature overnight. Et_2O (100 mL) was added to the mixture and it was extracted with an aqueous 1M K_2CO_3 solution (3 x 100 mL), with an aqueous 1M HCl solution (3 x 100 mL), and with a saturated aqueous NaCl solution (100 mL). The organic layer was dried over $MgSO_4$ and the solvent was removed on a rotary evaporator. The resultant residue was purified by column chromatography on silica gel (cyclohexane/EtOAc 8:2). Product **4** was isolated as a white solid in 81 % yield (10.6 g, 67.0 mmol).

^{1}H NMR (300 MHz, $CDCl_3$): δ (ppm) = 2.58 (s, 1H); 4.84 (d, J = 1.5 Hz, 2H); 7.00 - 7.15 (m, 2H); 7.55 (ddd, J = 1.7, 7.2, 8.8 Hz, 1H); 7.84 (dd, J = 1.8, 7.5 Hz, 1H); 10.47 (s, 1H). **^{13}C NMR** (75 MHz, $CDCl_3$): δ (ppm) = 56.7, 76.5, 77.7, 113.2, 121.6, 125.5, 128.5, 135.7, 159.7, 189.4. **HRMS** (ESI) m/z: $[(M+Na)^+]$ ($C_{10}H_8O_2Na$) calc.: 183.0417, found: 183.0414.

Compound **2** [28] (Scheme 3)

< Scheme 3>

8-Hydroxyjulolidine (2.4 g, 12.7 mmol) and trifluoromethanesulfonic acid (160 µL, 1.8 mmol) were added to a solution of benzaldehyde **4** (1.0 g, 6.3 mmol) in anhydrous dichloromethane (60 mL). The reaction was protected from light and it was stirred under argon at room temperature for 6 h. Then, tetrachloro-*p*-benzoquinone (1.5 g, 6.1 mmol) was added to the reaction mixture and the solution was stirred overnight still protected from light. The solvent was evaporated on a rotary evaporator and the resultant residue was purified by column chromatography on silica gel (CH_2Cl_2/MeOH/CF_3COOH 190:10:1). To obtain as pure product as possible, only very pure part of fractions was collected. Compound **2** was isolated as a purple solid in 8 % yield (0.3 g, 0.5 mmol).

^{1}H NMR (300 MHz, $CDCl_3$): δ (ppm) = 1.86 - 1.96 (m, 4H); 1.99 - 2.09 (m, 4H); 2.44 (t, J = 2.3 Hz, 1H); 2.63 (t, J = 5.8 Hz, 4H); 2.97 (t, J = 6.4 Hz, 4H); 3.33 - 3.56 (m, 8H); 4.56 (d, J = 2.4 Hz, 2H); 6.70 (s, 2H); 7.09 (dd, J = 1.7, 7.4 Hz, 1H); 7.12 - 7.23 (m, 2H); 7.48 - 7.58 (m, 1H). **^{13}C NMR** (75 MHz, $CDCl_3$): δ (ppm) =19.7, 19.9, 20.6, 27.6, 50.5, 50.9, 55.5, 76.0, 77.9, 105.1, 113.1, 121.7, 121.9, 123.5, 126.7, 131.0, 131.3, 151.1, 152.3, 154.2. **HRMS** (ESI) m/z: [M^+] ($C_{34}H_{33}N_2O_2$) calc.: 501.2537, found: 501.2525.

Compound **3** [28] (Scheme 4)

< Scheme 4>

A solution of $CuSO_4$ (7.3 mg, 29.2 µmol) and sodium ascorbate (6.7 mg, 33.8 µmol) in H_2O (1 mL) was added to a solution of rhodamine **2** (30.0 mg, 48.8 µmol) and 3-azido-1-propanol (23 µL, 249.1 µmol) in DMF (9 mL). The mixture was stirred at room temperature overnight and the solvents were evaporated. The residue was dissolved in CH_2Cl_2 (50 mL) and washed with 0.1 M Na_2EDTA aqueous solution (2 x 20 mL). The organic layer was dried over $MgSO_4$ and the solvent was removed on a rotary evaporator. The resultant residue was purified by column chromatography on silica gel (CH_2Cl_2 /EtOH/CF_3COOH 900:100:1). Compound **3** was isolated as purple oil in 57 % yield (20 mg, 28 µmol).

^{1}H NMR (300 MHz, $CDCl_3$): δ (ppm) = 1.78 - 2.17 (m, 8H); 2.19 - 2.34 (m, 2H); 2.50 - 2.75 (m, 4H); 2.84 - 3.12 (m, 4H); 3.29 - 3.56 (m, 8H); 4.20 - 4.33 (t, J = 6.2 Hz, 2H); 4.32 - 4.48 (m, 2H); 5.02 - 5.12 (m, 2H); 6.65 (s, 2H); 6.96 - 7.15 (m, 2H); 7.27 - 7.41 (m, 1H); 7.45 - 7.59 (m, 2H). **^{13}C NMR** (75 MHz, $CDCl_3$): δ (ppm) = 19.7, 19.9, 20.7, 27.6, 28.7, 46.6, 50.4, 50.9, 62.0, 65.0, 105.1, 113.2, 113.3, 113.4, 121.1, 121.8, 123.5, 124.5, 126.7, 130.6, 131.6, 142.5, 151.1, 152.3, 152.9, 155.4, 160.1, 160.6. **HRMS** (ESI) m/z: [M^+] ($C_{37}H_{40}N_5O_3$) calc.: 602.3126, found: 602.3129.

3. Results and discussion

3.1. Electrochemical and spectroelectrochemical investigation of rhodamine derivatives 1 and 2

Compounds **1** and **2** were first investigated to probe the fundamental electrochemical and spectroscopic properties of rhodamine 101 derivatives as well as to examine effects of an alkyne moiety on their behavior.

3.1.1. Electrochemistry

Cyclic voltammetry was used to investigate the electrochemical behavior of compounds **1** and **2** (Figure 1).

< Figure 1>

Both compounds exhibited a first reversible reduction process ($E^0_{\mathbf{1}}$ = -1.15 V, $E^0_{\mathbf{2}}$ = -0.97 V with E^0 determined from $(E_{pa} + E_{pc})/2$ where E_{pa} and E_{pc} are the anodic and cathodic peak potential values, respectively) and a second irreversible one ($E_{1R'}$ = -1.90 V, $E_{2R'}$ = -1.71 V). Compared to reported electrochemical behavior of rhodamine derivatives in aqueous solutions [22], no adsorption behavior of either **1** or **2** on the electrode surface appeared on the cyclic voltammograms shown in Figure 1 when acetonitrile was used as the solvent. The peak-to-peak separation measured in both cases for the first reversible reduction process ($\Delta Ep \sim 70$ mV) approaches theorical value of 59 mV and corresponds to the peak-to-peak separation of ferrocene oxidation measured under the same conditions which is consistent with a mono-electronic transfer (Figure 1a). Importantly, the presence of an alkyne moiety in compound **2** did not affect its fundamental electrochemical behavior compared to **1**. Nevertheless, replacement of the carboxylate moiety in **1** with a neutral alkyne fragment made the compound **2** easier to reduce compared to **1**. This result is in agreement with the lower electronic density of compound **2**. Based both on previously reported results [20-23] and our observations, it was possible to propose a mechanistic frame for rhodamine 101 electro-reductive behavior. Within the time-scale of cyclic voltammetry, the first electron transfer to **1** and **2** leads to the formation of radical species **1a** and **2a**, which are sufficiently stable to be either re-oxidized or further reduced into their corresponding anions **1b** and **2b**. The irreversibility of the second reduction waves suggests that anions **1b** and **2b** engage in a subsequent chemical reaction, most likely protonation (Scheme 5).

< Scheme 5>

3.1.2. UV-Vis Spectroelectrochemistry

Photophysical properties of rhodamine derivatives investigated in this work are summarized in Table 1. In the absence of applied potential, compounds **1** and **2** showed maximum absorption bands at 562 nm and 582 nm, respectively (Figure 2).

< Figure 2>

When potentials were applied, corresponding to the formation of radicals **1a** (-1.5 V/SCE) and **2a** (-1.4 V/SCE) (Scheme 5), original absorption bands of **1** and **2** disappeared and were replaced by new bands at 434 nm and 440 nm, respectively (Figures 2a, 2b). These changes agreed with visual observation as the starting pink solutions turned yellow.

To confirm that the newly formed peak at 440 nm could be assigned to the corresponding radical **2a,** TD-DFT calculations were performed on both the starting compound **2** and its reduced species **2a**. As shown in Figure 2c, the calculated absorption spectra ($\lambda_{max_\mathbf{2}_calc}$ = 556 nm, $\lambda_{max_\mathbf{2a}_calc}$ = 452 nm) were

in good agreement with the experimental ones ($\lambda_{max_\mathbf{2}_exp}$ = 582 nm, $\lambda_{max_\mathbf{2a}_exp}$ = 440 nm). This confirmed that absorption bands appearing at 434 nm and 440 nm can be assigned to the formation of the corresponding radical species **1a** and **2a**. However, and as shown in Figure 2c, the predicted intensity for **2a** was higher than that obtained experimentally. Also, the band intensity of **2a** was much lower compared to that of **1a** (Figures 2a, 2b).

When potentials, corresponding to the formation of anions **1b** (- 2 V/SCE) and **2b** (- 1.8 V/SCE), were applied, no new bands appeared (Figures 2a, 2b). This behavior was also in agreement with the visual evolution of solutions which totally decolorized confirming that reduction products did not absorb in the visible range.

The spectroelectrochemical investigations, led us to examine first the ability of compound **1** to be repeatedly and reversibly electrochemically switched between the reduced and the oxidized states. Absorbance intensity was recorded during application of a double potential step triggering successively the reduction of **1** into **1a** and the reoxidation of the latter back into the parental form **1**. Absorbance intensities were registered at wavelengths corresponding to absorption maxima of **1** (560 nm) or **1a** (435 nm). As shown in Figure 2d, the absorbance of **1** rapidly decreased during the reduction step, but was fully recovered in the second step (reoxidation). As expected, a symmetrical situation was observed for the electrogenerated radical species. Absorbance of **1a** (435 nm) rapidly increased upon the reduction step whereas it decreased during the reoxidation step. Importantly, no noticeable changes in absorbance intensities were observed after several cycles confirming the stability of the electrogenerated radical under these conditions. It is noteworthy that durations of reoxidation steps were ca. three times longer than reduction steps to allow complete diffusion of electrogenerated **1a** back to the electrode. Interestingly, a similar behavior was obtained with **2** indicating the electrogenerated radical **2a** was also stable under these conditions (Figure 2e).

3.1.3. Electrofluorochromism

Fluorescence spectroelectrochemical measurements were performed using the same spectroelectrochemical cell and the same methodology as for absorption. At open circuit potential, the emission spectra of **1** and **2** displayed an intense fluorescence peak at 599 nm (λ_{exc} = 566) and 614 nm (λ_{exc} = 580), respectively (Figures 3a, 3b).

< Figure 3>

During electrolysis, at potential values corresponding to the formation of radical forms (-1.3 V for **1** and -1.2 V for **2**), the fluorescence emission intensity disappeared in both cases within three minutes indicating that electrogenerated radicals **1a** and **2a** were non-fluorescent.

To confirm these results, fluorescence spectra were also recorded under excitations at 435 nm and 440 nm, which corresponded to the radical absorption wavelengths. Under these conditions, only residual fluorescence of initial rhodamine derivatives **1** and **2** was observed at open circuit potential (Figures 3c, 3d). During electrolysis, residual fluorescence rapidly disappeared and no new significant fluorescent signals appeared confirming that radicals **1a** and **2a** were non-fluorescent.

In this context, it was interesting to investigate the possible electrochemical fluorescence on/off switching between the rhodamine derivatives **1** and **2** and their corresponding non-fluorescent radicals **1a** and **2a**. Our first experiments were performed on compound **1**. Similarly to absorption

experiments, the spectroelectrochemical fluorescence response was recorded upon application of a double potential step triggering the reduction of **1** into its corresponding non-fluorescent radical **1a** and reoxidation into the fluorescent form **1**. Fluorescence intensity variations were registered at 599 nm (λ_{exc} = 566 nm). As shown in Figure 3e, a full ON/OFF switching could be achieved between the fluorescent oxidized and the non-fluorescent reduced states without noticeable loss of overall intensity during several cycles. Here again, the second potential step had to be around three times longer than the first reduction step to allow full diffusion-controlled reoxidation of **1a**. When the same experiment was performed with compound **2**, the fluorescence recovery upon switching was less efficient, (not shown).

3.2. Electrochemical and spectroelectrochemical investigations of compound 3

After exploring the electrochemical and spectroscopic properties of compounds **1** and **2** and showing the reversible electrofluorochromic properties of the former, our next objective was the modification of compound **2**, using the alkyne fragment, to examine whether the reversible electrochemical fluorescence switching observed with **1** could be restored. Accordingly, the triazole derivative **3** (Scheme 1) was prepared from **2**.
The UV-Vis and fluorescence spectra of **3** were first investigated (Figure 4a).

< Figure 4>

The substitution of the carboxylate moiety by a triazole group bearing an alkyl chain with an alcohol function did not significantly change the photophysical properties of **3** compared to **1** (Table 1). Nevertheless, the molar absorption coefficient of **1** was found to be nearly twice the value of that of **3** whereas the quantum yield of the latter was found to be slightly lower compared to **1**.
The electrochemical behavior of **3** was investigated by cyclic voltammetry. As shown in Figure 4b, the electrochemical reduction of **3** exhibited a reversible reduction wave ($E^0_{\mathbf{3}}$ = -0.96 V) located at a potential value close to that of compound **2** confirming the reduction potential dependence of rhodamine compounds upon electronic effects brought by substituents. By analogy to the previous investigations, the electrochemical reduction of **3** produced a radical species **3a** which appeared stable on the time-scale of cyclic voltammetry. As for **1** and **2**, the reduction of the electrogenerated radical **3a** was observed at a more negative potential value (-1.65 V; not shown).
During electrolysis, at a potential value corresponding to the formation of the radical species **3a** (-1.1 V), the fluorescence emission intensity of **3** decreased rapidly and fully switched after two minutes indicating that **3a** was non-fluorescent (Figure 4c). Importantly, fluorescence emission could be almost fully recovered by switching the applied potential to a value allowing reoxidation of the electrogenerated species demonstrating its electrofluorochromic properties (Figure 4d).

4. Conclusion

The photophysical and electrochemical properties of various rhodamine 101 derivatives have been investigated. The commercially available Rh101 (**1**), used as a reference model, was first examined. Contrary to its parental molecule, the electrogenerated radical form of Rh101 was found to be non-fluorescent. It was shown that the electrochemical fluorescence switching between the starting fluorescent Rh101 compound and its corresponding non-fluorescent radical form could be

achieved. This result prompted us to modify the Rh101 molecule with an alkyne moiety and investigate the electrochemical fluorescence properties of the new derivative **2**. Subsequently, it was used for the synthesis of the triazole derivative **3**. While the reversibility of electrochemical fluorescence switching in compound **2** was not as efficient as in compound **1,** fluorescence of compound **3** could be restored electrochemically, a most interesting feature for rhodamine-based compounds obtained by click chemistry. This work proved that rhodamine 101 derivatives can act both as light emitters and redox switches, opening new perspectives in the development of these fluorophores as practical probes, namely in fluorescence confocal microscopy [29].

Acknowledgements

This work was supported by EU Research and Innovation programme Horizon 2020 through the Marie Skłodowska-Curie action (H2020-MSCA-IF-2014, ID 6565190). The authors also thank to CNRS (UMR 8640 - PASTEUR), the French Ministry of Research, the Ecole Normale Supérieure, and Université P. et M. Curie.

References

[1] P. Audebert, F. Miomandre, Electrofluorochromism: from molecular systems to set-up and display, Chem. Sci. 4 (2013) 575-584.

[2] H. Al-Kutubi, H. R. Zafarani, L. Rassaei, K. Mathwig, Electrofluorochromic systems: Molecules and materials exhibiting redox-switchable fluorescence, *Eur. Polym. J.* 83 (2016) 478-498.

[3] F. Miomandre, C. Allain, G. Clavier, J.-F. Audibert, R. B. Pansu, P. Audebert, F. Hartl, Coupling thin layer electrochemistry with epifluorescence microscopy: An expedient way of investigating electrofluorochromism of organic dyes, *Electrochem. Commun.* 13 (2011) 574-577.

[4] Y. Kim, E. Kim, G. Clavier, P. Audebert, New tetrazine-based fluoroelectrochromic window; modulation of the fluorescence through applied potential, *Chem. Commun*. (2006) 3612-3614.

[5] M. Dias, P. Hudhomme, E. Levillain, L. Perrin, Y. Sahin, F.-X. Sauvage, C. Wartelle, Electrochemistry coupled to fluorescence spectroscopy: a new versatile approach, *Electrochem. Commun*. 6 (2004) 325-330.

[6] T. Suzuki, A. Migita, H. Higuchi, H. Kawai, K. Fujiwara, T. Tsuji, A novel redox switch for fluorescence: drastic UV-vis and fluorescence spectral changes upon electrolysis of a hexaphenylethane derivative of 10,10 '-dimethylbiacridan, *Tetrahedron Lett*. 44 (2003) 6837-6840.

[7] C. Quinton, V. Alain-Rizzo, C. Dumas-Verdes, F. Miomandre, G. Clavier, P. Audebert, Redox- and Protonation-Induced Fluorescence Switch in a New Triphenylamine with Six Stable Active or Non-Active Forms, *Chem. Eur. J*. 21 (2015) 2230-2240.

[8] G. Hennrich, H. Sonnenschein, U. Resch-Genger, Redox switchable fluorescent probe selective for either Hg(II) or Cd(II) and Zn(II), *J. Am. Chem. Soc.* 121 (1999) 5073-5074.

[9] G. Zhang, D. Zhang, X. Guo, D. Zhu, A new redox-fluorescence switch based on a triad with tetrathiafulvalene and anthracene units, *Org. Lett*. 6 (2004) 1209-1212.

[10] R. Martínez, I. Ratera, A. Tárraga, P. Molina, J. Veciana, A simple and robust reversible redox-fluorescence molecular switch based on a 1,4-disubstituted azine with ferrocene and pyrene units, *Chem. Commun*. (2006) 3809-3811.

[11] F. Montilla, I. Pastor, C. R. Mateo, E. Morallón, R. Mallavia, Charge transport in luminescent polymers studied by in situ fluorescence spectroscopy, *J. Phys. Chem. B.* 110 (2006) 5914-5919.

[12] M. Beija, C. A. Afonso, J. M. G. Martinho, Synthesis and applications of Rhodamine derivatives as fluorescent probes, *Chem. Soc. Rev.* 38 (2009) 2410-2433.

[13] R. P. Haugland in *A Guide to Fluorescent Probes and Labelling Technologies*, Invitrogen, Carlsbad, (2005) 11-37.

[14] M. Sameiro, M. S. T. Gonçalves, Fluorescent Labeling of Biomolecules with Organic Probes, *Chem. Rev.* 109 (2009) 190-212.

[15] G. T. Hermanson in *Bioconjugate Techniques*, Academic Press, Amsterdam, (2008) 415-430.

[16] A. M. Brouwer, Standards for photoluminescence quantum yield measurements in solution (IUPAC Technical Report), *Pure Appl. Chem*. 83 (2011) 2213-2228.

[17] A. J. Frank, J. W. Otvos, M. Calvin, QUENCHING OF RHODAMINE-101 EMISSION IN METHANOL AND IN COLLOIDAL SUSPENSIONS OF LATEX-PARTICLES, *J. Phys. Chem*. 83 (1979) 716-722.

[18] E. Bozkurt, M. Acar, Y. Onganer, K. Meral, Rhodamine 101-graphene oxide composites in aqueous solution: the fluorescence quenching process of rhodamine 101, *Phys. Chem. Chem. Phys*. 16 (2014) 18276-18281.

[19] M. Bossi, V. Belov, S. Polyakova, S. W. Hell, Reversible red fluorescent molecular switches, *Angew. Chem. Int. Ed.* 45 (2006) 7462-7465.

[20] A. M. Collins, X. Zhang, J. J. Scragg, G. J. Blanchard, F. Marken, Triple Phase Boundary Photovoltammetry: Resolving Rhodamine B Reactivity in 4-(3-Phenylpropyl)-Pyridine Microdroplets, *ChemPhysChem*. 11 (2010) 2862-2870.

[21] J. M. Austin, I. R. Harrison, T. I. Quickenden, ELECTROCHEMICAL AND PHOTOELECTROCHEMICAL PROPERTIES OF RHODAMINE-B, *J. Phys. Chem.* 90 (1986) 1839-1843.

[22] J.-S. Yu, T.-Y Zhou, The electrochemistry and thin-layer luminescence spectroelectrochemistry of rhodamine 6G at a 4,4 '-bipyridine-modified gold electrode, *J. Electroanal. Chem.* 504 (2001) 89-95.

[23] U. Krüger, R. Memming, FORMATION AND REACTIONS OF LONG LIVED XANTHENE DYE RADICALS .3. SPECTROELECTROCHEMICAL INVESTIGATIONS ON REDUCTION OF XANTHENE DYES, *Ber. Bunsen-Ges. Phys. Chem*. 78 (1974) 685-692.

[24] G. Baier, J.M. Siebert, K. Landfester, A. Musyanovych, Surface Click Reactions on Polymeric Nanocapsules for Versatile Functionalization, *Macromolecules*, 45 (2012) 3419-3427.

[25] R. R. Gagne, C. A. Koval, G. C. Lisensky, FERROCENE AS AN INTERNAL STANDARD FOR ELECTROCHEMICAL MEASUREMENTS, *Inorg. Chem*. 19 (1980) 2854-2855.

[26] M. J. Frisch, G. W. Trucks, H. B. Schlegel, G. E. Scuseria, M. A. Robb, J. R. Cheeseman, G. Scalmani, V. Barone, B. Mennucci, G. A. Petersson, H. Nakatsuji, M. Caricato, X. Li, H. P. Hratchian, A. F. Izmaylov, J. Bloino, G. Zheng, J. L. Sonnenberg, M. Hada, M. Ehara, K. Toyota, R. Fukuda, J. Hasegawa, M. Ishida, T. Nakajima, Y. Honda, O. Kitao, H. Nakai, T. Vreven, J. A. Montgomery, Jr., J. E. Peralta, F. Ogliaro, M. Bearpark, J. J. Heyd, E. Brothers, K. N. Kudin, V. N. Staroverov, R. Kobayashi, J. Normand, K. Raghavachari, A. Rendell, J. C. Burant, S. S. Iyengar, J. Tomasi, M. Cossi, N. Rega, J. M. Millam, M. Klene, J. E. Knox, J. B. Cross, V. Bakken, C. Adamo, J. Jaramillo, R. Gomperts, R. E. Stratmann, O. Yazyev, A. J. Austin, R. Cammi, C. Pomelli, J. W. Ochterski, R. L. Martin, K. Morokuma, V. G. Zakrzewski, G. A. Voth, P. Salvador, J. J. Dannenberg, S. Dapprich, A. D. Daniels, O. Farkas, J. B. Foresman, J. V. Ortiz, J. Cioslowski, and D. J. Fox, Gaussian 09, Revision A.02, Gaussian, Inc., Wallingford CT, (2009).

[27] F. Birbaum, A. Neels, C. G. Bochet, Photochemistry of allenyl salicylaidehydes, *Org. Lett.* 10 (2008) 3175-3178.

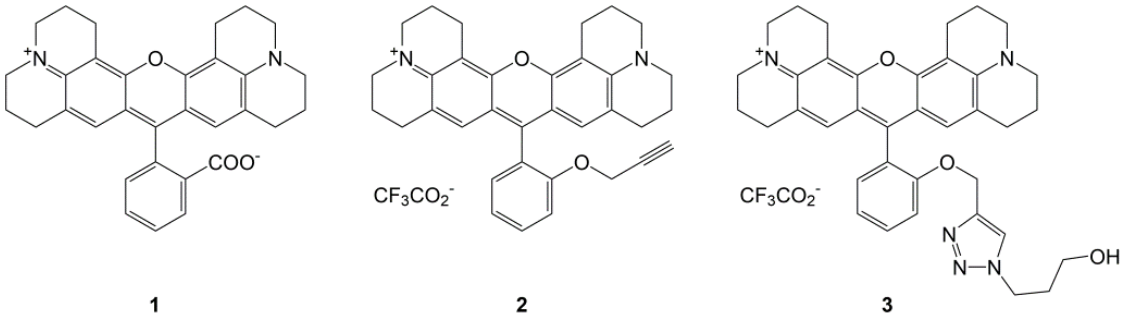
[28] G. Despras, A.I. Zamaleeva, L. Dardevet, C. Tisseyre, J.G. Magalhaes, C. Garner, M. de Waard, S. Amigorena, A. Feltz, J.-M. Mallet, M. Collot, H-Rubies, a new family of red emitting fluorescent pH sensors for living cells, *Chem. Sci*. 6 (2015) 5928-5937.

[29] A. I. Perez Jimenez, L. Challier, E. Aït-Yahiatène, J. Delacotte, E. Labbé, O. Buriez, Selective Electrochemical Bleaching of the Outer Leaflet of Fluorescently Labeled Giant Liposomes, *Chem. Eur. J.* 23 (2017) 6781 – 6787.

Schemes, Figures and Table

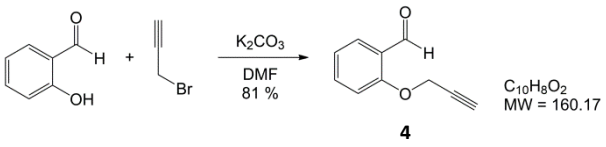
SCHEMES:

Scheme 1. Chemical structures of rhodamine 101 (**1**), alkyne **2** and triazole **3** derivatives investigated in this work.



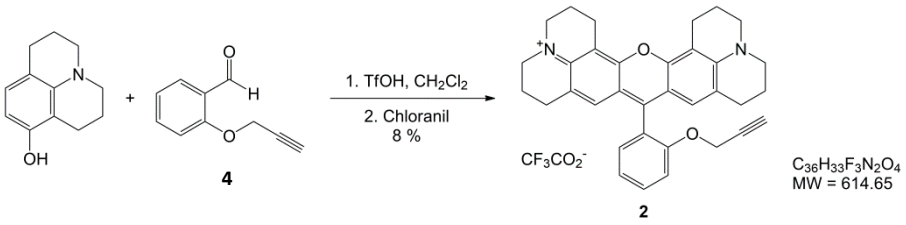
1 **2** **3**

Scheme 2.



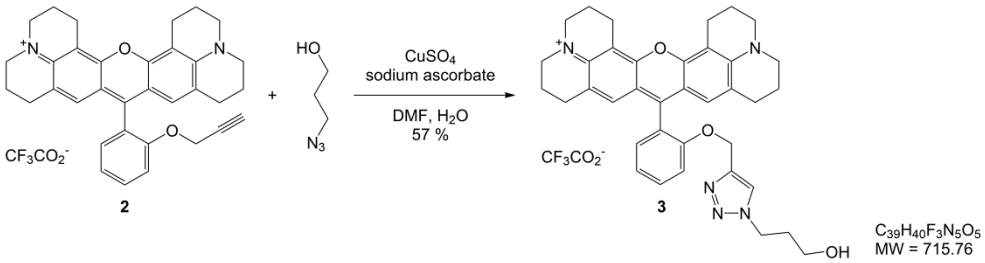
4

Scheme 3.



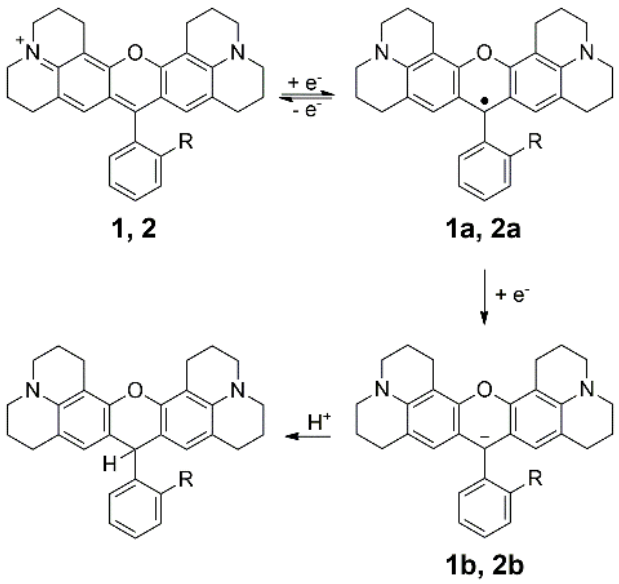
4 2

Scheme 4.



2 3

Scheme 5. General electrochemical reduction scheme for rhodamine derivatives **1** (R = COO^-) and **2** (R = $OCH_2C{\equiv}CH$)



FIGURES

Figure 1. Cyclic voltammograms of **1** (0.2 mM) and **2** (0.2 mM) in MeCN / [TBA][BF_4](0.1 M), performed at a scan rate of 200 mV/s and at a glassy carbon electrode; (a) first reversible reduction process; (b) full scan.

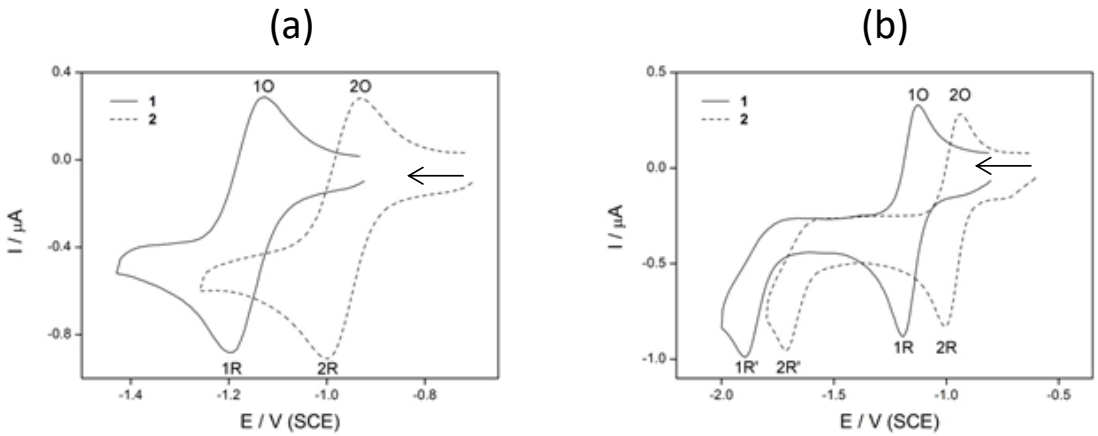


Figure 2. Absorption spectra of a) **1** (0.08 mM) and b) **2** (0.08 mM) recorded in TBA·BF_4/MeCN (0.1 M) before (solid lines) and after their *in situ* electrochemical reduction (for 2 minutes) at potential values corresponding to the formation of radicals (dashed lines) **1a**, **2a** and anions (dotted lines) **1b**, **2b**. c) Comparison of experimental (exp) and calculated (cal) absorption spectra of compound **2** and its radical form **2a**. d) Absorbance switching responses of the starting compound **1** recorded at 560 nm and of its corresponding electrogenerated species **1a** monitored at 435 nm. Switching potential values and step duration times were as follows: E_{red} = -1.4 V (10 s), E_{ox} = -0.2V (30 s) for both **1** and **1a.** e) Absorbance switching responses of compound **2** recorded at 580 nm and of its corresponding electrogenerated species **2a** monitored at 440 nm. Switching potential values and step duration times were as follows: E_{red} = -1.2 V (7 s), E_{ox} = -0.2V (30 s) for both **2** and **2a.**

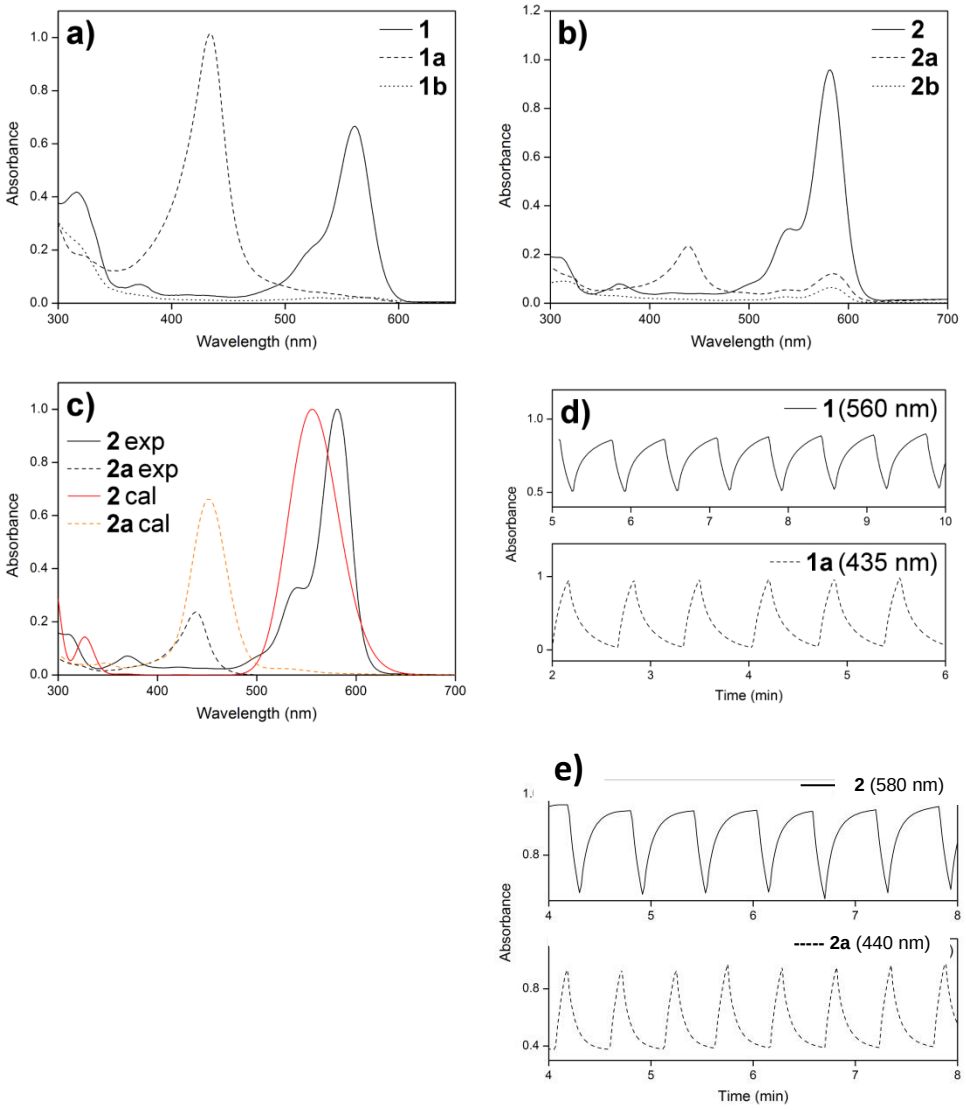


Figure 3. Time evolution of fluorescence emission spectra recorded in TBA·BF_4/MeCN (0.1 M) at electrode potentials of -1.3 V for **1** and -1.2 V for **2**; a) **1** (0.08 mM, λ_{exc} = 566 nm); b) **2** (0.08 mM, λ_{exc} = 580 nm); c) **1a** (0.08 mM, λ_{exc} = 440 nm); d) **2a** (0.08 mM, λ_{exc} = 435 nm); e) Reversible fluorescence switching of compound **1** monitored at 599 nm (λ_{exc} = 566 nm). Switching potential values and step duration times were as follows: E_{red} = -1.3 V (10 s), E_{ox} = -0.5 V (30 s).

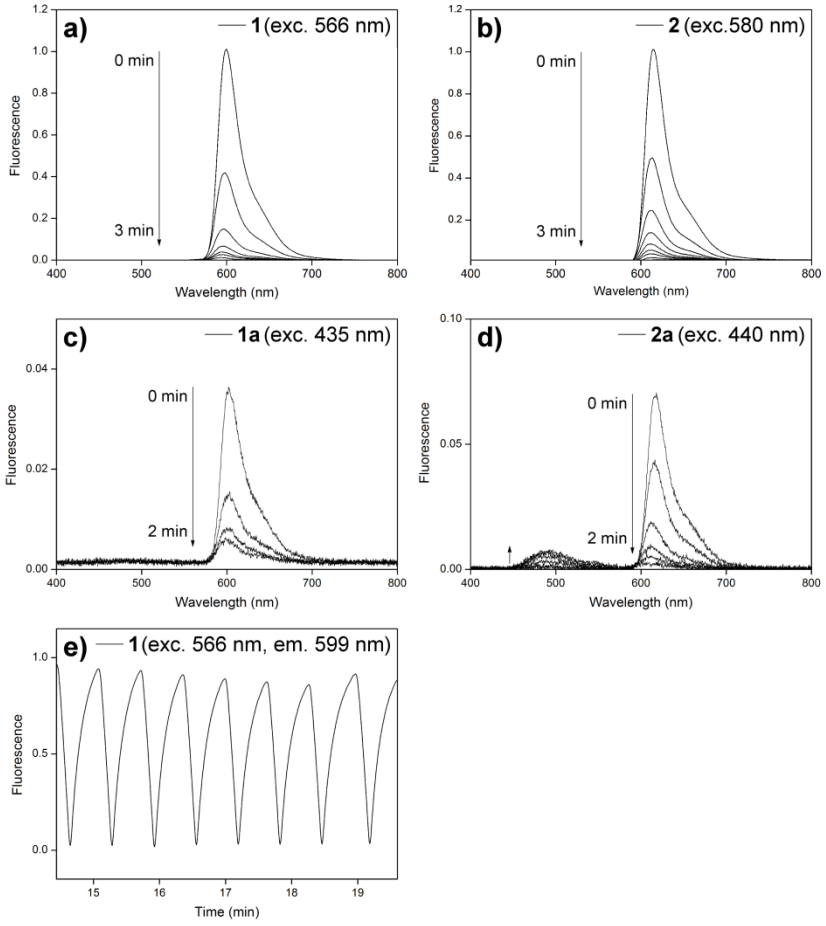
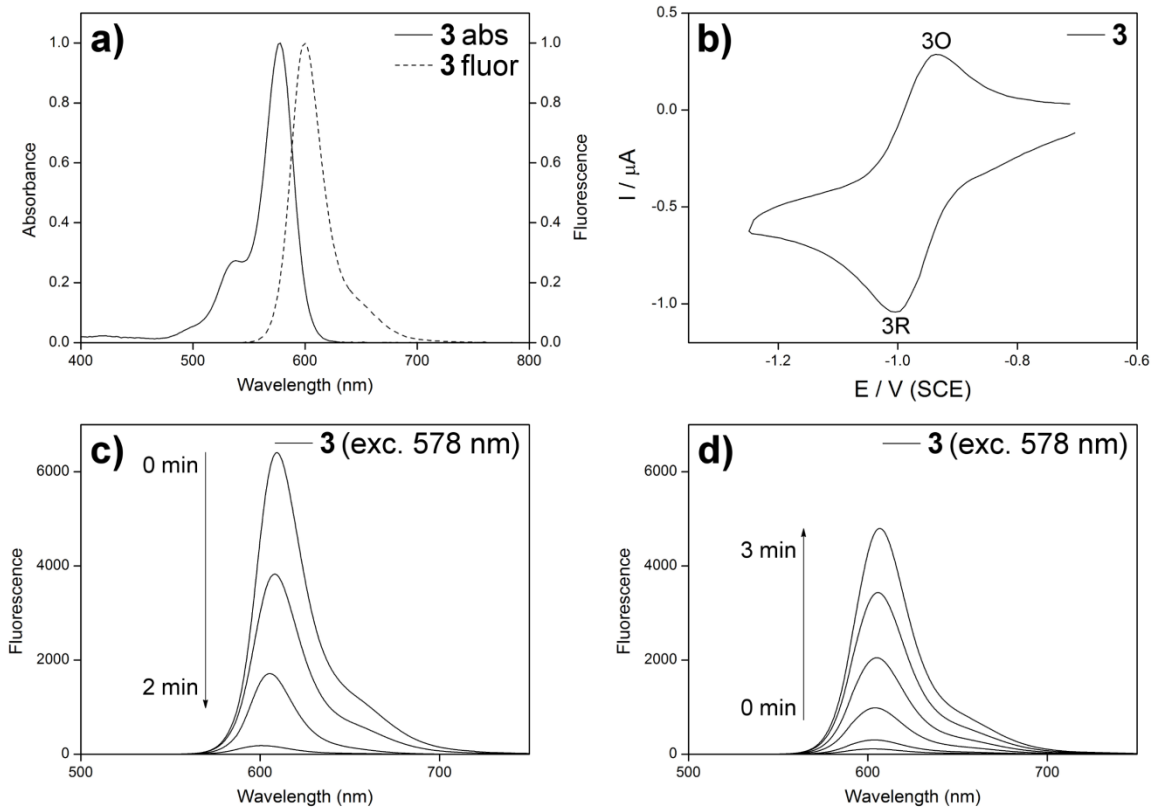


Figure 4. a) Absorption and fluorescence spectra of **3** in MeCN; b) Cyclic voltammogram of **3** (0.5 mM) in TBA·BF_4/MeCN (0.1 M), performed at a scan rate of 200 mV/s at a glassy carbon electrode; c) Fluorescence emission spectra recorded upon reduction of **3** at -1.1 V and d) upon reoxidation of the electrogenerated **3a** species at +0.3 V (λ_{exc} = 578 nm); time evolution of fluorescence emission spectra shown in d) have been performed just after c) (same experiment).



TABLE

Table 1. Photophysical properties of rhodamine derivatives.

Compound	λ_{abs} [nm]	ε [L mol^{-1} cm^{-1}]	λ_{em} [nm]	Φ
1	566[a]	109 100	593	1.00 [16]
	562[b]	-	-	-
1a	434[b]	-	-	-
2	580[a]	153 700	614	0.89
	582[b]	-	-	-
2a	440[b]	-	-	-
3	578[a]	64 000	600	0.76

[a]Measured in MeOH, [b]Measured in MeCN + TBA.BF4 (0.1 M).